Nonhyperbolic moveout inversion of qP-waves in layered VTI media using rational interpolation

Huub Douma[1] and Mirko van der Baan[2]
[1] *Center for Wave Phenomena, Colorado School of Mines, Golden, CO 80401-1887, USA*
[2] *University of Leeds, School of Earth Sciences, Leeds LS2 9JT, United Kingdom*

ABSTRACT
The nonhyperbolic moveout observed in common-midpoint gathers is often ascribed to the presence of seismic anisotropy in the subsurface. Therefore, this moveout is commonly used to get (initial) estimates of the relevant seismic parameters describing such anisotropy. For qP-waves in laterally homogeneous transversely isotropic media with a vertical symmetry axis (VTI), these parameters are the anellipticity parameter η and the zero-dip normal moveout velocity V_{nmo}. The τ-p domain is the natural domain for parameter estimation in horizontally layered media since cusps do not occur in this domain and because the horizontal slowness is preserved upon propagation. However, the need for methods that use the τ-p domain to transform the data or to pick traveltimes in the x-t domain, is a practical disadvantage. To overcome this, we combine a τ-p domain inversion technique with rational interpolation of traveltimes in the x-t domain. This combination results in a highly accurate, yet efficient semblance-based method in the x-t domain, for estimating the interval values of η and V_{nmo} from the moveout of qP-waves reflected once in a horizontally layered VTI medium. The efficiency of the method stems from the fact that rational interpolation needs only few (here five) support points to obtain accurate moveout interpolation. The accuracy of the method is verified with a numerical example.

Key words: nonhyperbolic moveout, qP-waves, anisotropy, parameter estimation, rational interpolation, semblance

Introduction

In the past two decades, seismic data processing has gradually developed to allow an estimate of seismic anisotropy to be obtained from the data. A common method to get (initial) estimates of seismic anisotropy is to analyze the nonhyperbolic part of the moveout in a CMP gather (Tsvankin & Thomsen, 1994; Alkhalifah & Tsvankin, 1995; Alkhalifah, 1997; Grechka & Tsvankin, 1998; Tsvankin, 2001Chapter 4). This analysis originated with the work of Hake *et al.* (1984), who presented a three-term Taylor expansion to describe the moveout in a CMP gather acquired over a horizontally-layered transversely isotropic (TI) medium. Tsvankin & Thomsen (1994) presented an improved rational approximation that provided better accuracy at long offsets, but many authors subsequently pointed out the lack of accuracy at intermediate offsets [e.g., Grechka & Tsvankin (1998), Zhang & Uren (2001), van der Baan & Kendall (2002), Stovas & Ursin (2004), and Douma & Calvert (2006)]. This observation led to several other methods, such as the $\tau - p$ based method (Van der Baan & Kendall, 2002; Van der Baan, 2004), the shifted-hyperbola-based approach [e.g., Fomel (2004)], continued-fraction-based approaches [e.g., Ursin & Stovas (2006)], and a rational-interpolation-based method (Douma & Calvert, 2006).

Because horizontal slowness is preserved upon propagation through horizontally layered media, and because traveltimes as a function of the horizontal slowness p are single-valued, the τ-p transform is the natural domain for anisotropy parameter estimation in layered media (Hake, 1986; Van der Baan & Kendall, 2002). Since the τ-p transform is a plane-wave decomposition, the relevant velocity is phase velocity rather than group velocity. The latter velocity is mathematically more complex and often follows from approximations to already approximated phase velocities. Hence, anisotropy-parameter estimation in the τ-p domain renders the extra approximation for the group velocity unnecessary, thus leading to more accurate estimates of the relevant parameters.

The disadvantage of the τ-p domain inversion technique is that we either need to (1) transform the x-t gathers to the τ-p domain and pick the τ-p curves in this domain, or (2) pick the $t(x)$ moveout curves using a least-squares fitting procedure and transform these to the τ-p domain. Most interpreters prefer the second option since they have more experience viewing data in the x-t domain (Van der Baan & Kendall, 2002). Manual picking of the moveout curves, however, is in practice cumbersome despite being prone to error.

The approximation to nonhyperbolic moveout of qP waves given by Tsvankin & Thomsen (1994) is a rational approximation that is exact at zero and infinite offset. Recognizing the accuracy of rational approximants together with the need for better accuracy at intermediate offsets, Ursin & Stovas (2006) recently derived a rational approximation (written as a continued fraction) for nonhyperbolic moveout in layered VTI media by matching a Taylor series expansion for the squared traveltime up to sixth order in offset (actually third order in squared offset); such approximation is also known as *Padé approximation* [e.g., Baker (1975) or Bender & Orszag (1978)]. Although this rational approximation provides improved accuracy at intermediate offsets, beyond certain offsets it loses accuracy. To overcome this, but at the same time recognizing the accuracy of the rational approximation, Douma & Calvert (2006) proposed a *rational interpolation* approach to describe nonhyperbolic moveout. In this method, the moveout is obtained through rational interpolation of traveltimes at offsets where accuracy is desired, i.e., at offsets acquired in the field. They showed that for a single horizontal VTI layer, the rational-interpolation-based method, using quadratic polynomials in both the numerator and the denominator, allows for highly accurate moveout correction up to offset-to-depth ratios of about 8, combined with unbiased estimation of V_{hor} (or η).

We extend the rational-interpolation-based method of Douma & Calvert (2006) to a horizontally layered TI medium with a vertical symmetry axis, based on nearly exact traveltimes derived from the τ-p curve in combination with the acoustic approximation of Alkhalifah (1998). This allows us to set up a three-parameter, i.e., t_0, η, and V_{nmo}, semblance-based analysis in the $t-x$ domain, to invert qP-wave moveout for the interval values of η and V_{nmo} as a function of the zero-offset two-way traveltime t_0, without the use of a Dix-type averaging procedure (Dix, 1955). The presented method is highly efficient due to a combination of expressions for the traveltimes and offsets that are explicit in the interval values of η and V_{nmo} and the horizontal slowness, and because rational interpolation needs only few support points (here five) to obtain accurate moveout interpolation. Since we are dealing with qP-waves only, interpolation can be done in the $x-t$ domain since no cusps can occur on qP wavefronts due to the convexity of the slowness surface of such waves. The method can be extended to pure mode qSV reflections based on the weak anisotropy approximation of the phase velocity for such waves (Thomsen, 1986), provided the measured reflected wavefront does not contain any cusps. In case the reflected wavefront does contain cusps, the $\tau-p$ domain is the natural domain of choice for horizontally layered media, as pointed out by van der Baan & Kendall (2002).

The organization of this paper is as follows. First, we review the $\tau-p$ curve and subsequently use it to develop the expressions for traveltime and offset of pure-mode qP reflected waves in layered VTI media, as a function of the horizontal slowness. We then proceed to present the rational-interpolation-based procedure for traveltime estimation, and explain its use in interval parameter estimation of η (or V_{hor}) and V_{nmo}. Finally, a numerical example illustrates the method.

The general $\tau-p$ curve

From simple geometric considerations, it follows that in an (anisotropic) homogeneous medium the horizontal distance $\Delta x'$ traveled by a plane wave within a time interval $\Delta t'$ is given by

$$\Delta x' = v_g^x \Delta t' \ , \tag{1}$$

where v_g^x is the horizontal group velocity. The length of the projection of the group-velocity vector on the normal to the wavefront equals the phase velocity [e.g. Vlaar (1968, p.23) or Helbig (1994)]. Therefore, in two dimensions,

$$p v_g^x + q v_g^z = 1 \ , \tag{2}$$

where p and q are the horizontal and vertical components of the slowness vector $\boldsymbol{p}$, respectively, and v_g^z is the vertical component of the group velocity. Using equation (2) in equation (1) and solving for $\Delta t'$ we have

$$\Delta t' = p\Delta x' + q\Delta z \ , \tag{3}$$

where we used $\Delta z = v_g^z \Delta t'$. The two-way traveltime Δt can be split into two one-way traveltimes $\Delta\acute{t}'$ and $\Delta\grave{t}'$ for the up- and down-going ray, respectively, i.e.,

$$\Delta\acute{t}' = \acute{p}\Delta x' - \acute{q}\Delta z, \quad \Delta\grave{t}' = \grave{p}\Delta x' + \grave{q}\Delta z \ , \tag{4}$$

where we denote explicitly the difference in the vertical direction for the up- and down-going rays. For a reflected wave in a horizontal layer, it follows, using Snell's law $\acute{p} = \grave{p} = p$, that

$$\Delta t = \Delta \acute{t}' + \Delta \grave{t}' = p\Delta x + (\grave{q} - \acute{q})\Delta z \; , \tag{5}$$

where $\Delta x = 2\Delta x'$ denotes the offset. Assuming that the medium has a horizontal symmetry plane (such as transversely isotropic media with either a vertical or a horizontal symmetry axis, or orthorhombic media with a horizontal symmetry plane, or even monoclinic media with a horizontal symmetry plane) and assuming pure-modes only (i.e., qP-waves, qSV-waves and qSH-waves), we have $\grave{q} = -\acute{q} = q$. Using this in equation (5) then gives

$$\Delta t = p\Delta x + 2q\Delta z \; . \tag{6}$$

Defining the intercept time $\Delta\tau := \Delta t - p\Delta x$, and replacing the single layer with a stack of homogeneous anisotropic horizontal layers, we obtain the $\tau - p$ curve [e.g., Chapman (2004, section 2.3)]

$$t = px + \tau \; , \tag{7}$$

with x denoting the offset and with

$$\tau = \sum_i \Delta t_0^i v_0^i q^i \; , \tag{8}$$

where t_0^i is the two-way vertical traveltime in layer i, and v_0^i and q^i are the vertical group velocity and vertical slowness in layer i, respectively. It follows from the definition of the $\tau - p$ curve that

$$\frac{d\tau}{dp} = -x \; . \tag{9}$$

Traveltimes for qP-waves in layered VTI media based on the $\tau - p$ curve

Although equation (7) is valid in generally anisotropic horizontally layered media with a horizontal symmetry plane, and valid for qP-waves as well as for qSV-waves and qSH-waves, we treat qP-waves in VTI media only. Since for such waves no cusps can occur in the moveout due to the convexity of the slowness surface, this allows the interpolation to be done in the $x - t$ domain. Also, in horizontally layered VTI media, each vertical plane is a symmetry plane, so the vertical group-velocity is the same as the vertical phase velocity. Therefore, the vertical group velocity v_0^i in equation (8) is replaced with the vertical phase velocity V_0^i (i.e., V_{P0}^i for qP-waves).

The traveltimes of qP-waves in laterally homogeneous VTI media depend mainly on the zero-dip normal-moveout velocity V_{nmo} and the anellipticity parameter η (Alkhalifah & Tsvankin, 1995). The vertical shear-wave phase velocity V_{S0} has negligible influence on the traveltimes of such waves in TI media (Tsvankin & Thomsen, 1994; Tsvankin, 1996; Alkhalifah, 1998). Alkhalifah (1998) derived an approximate relation for the vertical slowness q in terms of V_{nmo} and η by setting $V_{S0} = 0$. This relation is given by

$$V_{P0}^2 q^2 = 1 - \frac{1 - p^2 V_{nmo}^2}{1 - 2\eta p^2 V_{nmo}^2} \; . \tag{10}$$

Setting $V_{S0} = 0$ is described as the acoustic approximation by Alkhalifah (1998). Grechka & Tsvankin (1998) showed that the horizontal velocity $V_{hor} = V_{nmo}\sqrt{1 + 2\eta}$ is better constrained from semblance-based moveout analysis than is η. Therefore, in anticipation of a semblance-based parameter estimation, we rewrite equation (10) in terms of V_{hor} and V_{nmo}. When we do this, equation (10) becomes

$$V_{P0}^2 q^2 = \frac{1 - p^2 V_{hor}^2}{1 - p^2 \left(V_{hor}^2 - V_{nmo}^2\right)} \; . \tag{11}$$

Using equation (11) in (8) then gives τ explicit in the relevant parameters V_{hor} and V_{nmo}, i.e.,

$$\tau = \sum_i \Delta t_0^i \sqrt{\frac{1 - p^2 \left(V_{hor}^i\right)^2}{1 - p^2 \left[\left(V_{hor}^i\right)^2 - \left(V_{nmo}^i\right)^2\right]}} \; . \tag{12}$$

With this expression we can calculate the derivative $d\tau/dp$ and use the resulting expression in equation (9) to find the offset x explicit in V_{hor} and V_{nmo}. Doing this gives

$$x = \sum_i \Delta t_0^i \left(\frac{p\left(V_{nmo}^i\right)^2 / \sqrt{1 - p^2 \left(V_{hor}^i\right)^2}}{\left\{1 - p^2 \left[\left(V_{hor}^i\right)^2 - \left(V_{nmo}^i\right)^2\right]\right\}^{3/2}} \right). \tag{13}$$

Finally, using equations (12) and (13) in (7), we get an expression for the traveltime as function of the horizontal slowness p explicit in the relevant parameters V_{hor}^i and V_{nmo}^i, i.e.,

$$\begin{aligned} t \;\; = \;\; & \sum_i \Delta t_0^i \left(\frac{p^2 \left(V_{nmo}^i\right)^2}{\left\{1 - p^2 \left[\left(V_{hor}^i\right)^2 - \left(V_{nmo}^i\right)^2\right]\right\}} \right. \\ & + \left.\left[1 - p^2 \left(V_{hor}^i\right)^2\right]\right) \left(\left[1 - p^2 \left(V_{hor}^i\right)^2\right] \right. \\ & \left. \left\{1 - p^2 \left[\left(V_{hor}^i\right)^2 - \left(V_{nmo}^i\right)^2\right]\right\} \right)^{-1/2} \; . \end{aligned} \tag{14}$$

The weak anisotropy approximation (Thomsen, 1986) can be used to linearize the phase velocity V_{SV} for qSV waves as a function of phase angle, which can subsequently be written [equation (31) from van der Baan & Kendall (2002)] in terms of the horizontal slowness as

$$\begin{aligned} V_{SV}(p) \;\; \approx \;\; & \left(-1 + 2\sigma p^2 V_{S0}^2 + \left\{\left(1 - 2\sigma p^2 V_{S0}^2\right)^2 \right.\right. \\ & \left.\left. + 8\sigma p^4 V_{S0}^4 \right\}^{1/2}\right) / \left(4\sigma p^4 V_{S0}^2\right) \; , \end{aligned} \tag{15}$$

with $\sigma := (V_{P0}/V_{S0})^2(\epsilon - \delta)$. Then the vertical slowness q can be found using $q^2 = 1/V_{SV}^2 - p^2$, which can subsequently be used in equation (8) to find the intercept time. Substitution of this result in equations (7) and (9) gives the equivalent expressions to equations (13) and (14) for the offsets and associated traveltimes of reflected qSV waves. The resulting expressions could be made explicit in the NMO velocity V_{nmo}^{SV} using the relation $V_{nmo}^{SV} = V_{S0}\sqrt{1+2\sigma}$. Such expressions could be used only in an $x-t$ based interpolation scheme provided the wavefront does not contain any cusps. Although such a treatment is possible, linearized approximations for qSV-waves are often not very accurate because the presence of the squared V_{P0}/V_{S0} in the definition of σ often makes σ much larger than ϵ and δ (Tsvankin, 2001p.26-27). Therefore we refrain from this treatment and subsequent numerical verification.

Rational interpolation

Equations (13) and (14) are explicit in p. For an x-t based semblance analysis, however, we require traveltimes for all offsets acquired in the field. Finding the p value associated with a certain offset x in equation (13) corresponds to a simplified 2-point ray-tracing problem, which can be solved using a straightforward bisection approach since the offset x and traveltime t in equations (13) and (14) are single-valued and monotonically increasing with increasing p-value. In principle this can be done for each available offset and the resulting moveout curves can be used to perform a semblance-based parameter estimation in the $x-t$ domain. Here, however, we propose a more elegant and computationally less demanding procedure that uses the traveltimes and offsets calculated for a few p-values only in the rational-interpolation-based approach of Douma & Calvert (2006). In this way, the method of Douma & Calvert, which is based on a single horizontal VTI layer, can be extended to horizontally layered VTI media. The proposed method naturally encompasses the single-layer case, hence removing the need for the tabulated approach used by Douma & Calvert.

A rational approximation to a function $t(x)$ is generally written as [e.g., Stoer & Bulirsch (1993, p.58-63)]

$$t(x) \approx \frac{N_L(x)}{D_M(x)} = \frac{n_0 + n_1 x + \cdots + n_L x^L}{d_0 + d_1 x + \cdots + d_M x^M}\,, \qquad (16)$$

with $N_L(x)$ a polynomial of order L, and $D_M(x)$ a polynomial of order M. We denote such an approximation as $[L/M]$. This rational approximation is determined by the $L+M+2$ unknown coefficients n_i, $i = 0, 1, \ldots, L$ and d_i, $i = 0, 1, \ldots, M$. Since these coefficients can be determined up to only a common factor $\rho \neq 0$, the $[L/M]$ rational approximation is fully determined by $L+M+1$ support points (x_i, t_i) satisfying

$$t(x_i) = \frac{N_L(x_i)}{D_M(x_i)} = t_i\,. \qquad (17)$$

Hence, it is necessary that the coefficients satisfy

$$N_L(x_i) - t_i D_M(x_i) = 0\,. \qquad (18)$$

Satisfying equation (18), however, is not a sufficient condition for equation (17) to hold since $N_L(x_i)$ and $D_M(x_i)$ may both be zero. In that case, the rational interpolation problem is unsolvable, and support points (x_i, t_i) cannot be reached and are thus missed by the rational function $N_L(x)/D_M(x)$. Such support points are usually referred to as *inaccessible.* If x_i is an inaccessible point, the functions $N_L(x)$ and $D_M(x)$ have (at least) a common factor $x - x_i$. If $N_L(x)$ and $D_M(x)$ have no such common factor, the rational interpolation problem is solvable (Stoer & Bulirsch, 1993p.58-63).

If the $L+M+1$ support points (x_i, t_i) of an $[L/M]$ rational approximant can be interpolated by a $[L'/M']$ rational approximation with $L'+M' < L+M$, the support points are said to be in *special position* (Stoer & Bulirsch, 1993p.61-62). Suppose $i_1, \ldots, i_\alpha$ are the subscripts of the inaccessible points of the $[L/M]$ rational approximant $t(x)$ in equation (16). Then, $N_L(x)$ and $D_M(x)$ have common factor $\Pi_{j\in\{i_1,\ldots,i_\alpha\}}(x-x_j)$, which after cancellation leaves an equivalent $[L'/M']$ rational approximant with $L'+M'+1 = L+M+1-2\alpha$. Since the remaining polynomials $N'_L(x)$ and $D'_M(x)$ have no more common factors, they form a rational approximation $t'(x) = N'_L(x)/D'_M(x)$ that solves the rational interpolation problem through the remaining $L+M+1-\alpha$ accessible points. Since $L+M+1-\alpha > L+M+1-2\alpha = L'+M'+1$, it follows that the accessible support points of a nonsolvable rational interpolation problem can always be interpolated by a $[L'/M']$ rational approximation with $L'+M' < L+M$, and are thus always in special position. This means that the nonsolvability of a rational interpolation problem is really a matter of degeneracy. Therefore, the possible nonsolvability of a rational interpolation problem is never an issue in practice, since it can be overcome by adding arbitrarily small perturbations to the support points.

If x and t in equation (16) denote squared offset and squared traveltime, respectively, it follows that for purely hyperbolic moveout all the support points are in special position. As shown in the Appendix A, this means that in that case the linear system (18) is degenerate. This was also noted by Douma & Calvert (2006), who observed that this degeneracy can be overcome by arbitrarily small perturbations (in the form of numerical noise) of the support points (x_j, t_j). If, however, x and t denote offset and time instead of squared offset and squared time, then there is no degeneracy for hyperbolic moveout. Here, we therefore interpolate the traveltimes as a function of offset as opposed to the squared traveltimes as a function of the squared offsets, as done by Douma & Calvert (2006).

Douma & Calvert explicitly solve the linear system (18) for [2/2] rational interpolation in their Appendix A. Alternatively, the rational approximant $N_L(x)/D_M(x)$ can be written as a Thiele continued fraction (Stoer &

Table 1. Model parameters used in ray-tracing to determine the traveltimes from a layered model. The associated CMP gather is shown in Figure 1a.

layer	h (m)	V_{nmo} (m/s)	V_{hor} (m/s)	η	V_{P0} (m/s)	V_{S0} (m/s)	ϵ	δ
1	1000	2098	2098	0.00	2000	300	0.050	0.05
2	2000	2000	2298	0.16	2000	300	0.160	0.00
3	3000	2892	3747	0.34	3048	300	0.255	-0.05
4	4000	2464	3882	0.74	3292	300	0.195	-0.22

Bulirsch, 1993, p.63-67) given by

$$\frac{N_L(x)}{D_M(x)} = t_0 + \frac{x-x_0}{\rho(x_0,x_1)+} \; \frac{x-x_1}{\rho(x_0,x_1,x_2)-\rho(x_0)+} \; \frac{x-x_{M+L-1}}{\rho(x_0,\ldots,x_{M+L})-\rho(x_0,\ldots,x_{M+L-2})} \,, \tag{19}$$

where we use the notation $\frac{a}{b+}\,\frac{c}{d} = \frac{a}{b+c/d}$. Here, the reciprocal differences ρ are defined by

$$\rho(x_i) := t_i \,, \tag{20}$$

$$\rho(x_i,x_k) := \frac{x_i-x_k}{t_i-t_k} \,, \tag{21}$$

$$\rho(x_i,x_{i+1},\ldots,x_{i+k}) := (x_i-x_{i+k})\,/ \, [\rho(x_i,\ldots,x_{i+k-1}) - \rho(x_{i+1},\ldots,x_{i+k})] + \rho(x_{i+1},\ldots,x_{i+k-1}) \,. \tag{22}$$

Here, we use the same order of rational interpolation that Douma & Calvert used, i.e., a [2/2] rational interpolation, since they showed that this order of interpolation (at least for a single horizontal homogeneous VTI layer) provides high accuracy in the traveltimes up until offset-to-depth ratios of 8. Setting $L = M = 2$ in equation (19) gives the resulting Thiele continued-fraction interpolation, i.e.,

$$\begin{aligned} t(x) &\approx \frac{N_2(x)}{D_2(x)} \\ &= t_0 + \frac{x-x_0}{\rho(x_0,x_1)+} \; \frac{x-x_1}{\rho(x_0,\ldots,x_2)-\rho(x_0)+} \; \frac{x-x_2}{\rho(x_0,\ldots,x_3)-\rho(x_0,x_1)+} \; \frac{x-x_3}{\rho(x_0,\ldots,x_4)-\rho(x_0,\ldots,x_2)} \,. \end{aligned} \tag{23}$$

This equation can be used to find the function values $t(x)$ at values of x different from the support abscissas x_i. Note that for the [2/2] rational interpolation *only four* support points need to be calculated, because t_0 is treated as a parameter, rendering the method highly efficient.

Three-parameter semblance-based parameter estimation in the $x - t$ domain

We use the expressions for the traveltimes and associated offsets, i.e., equations (14) and (13), respectively, to calculate the support points for the rational interpolation. That is, given four p-values p_j $(j = 1,\ldots,4)$, and given the model parameters Δt_0^i, V_{hor}^i, and V_{nmo}^i, we calculate the pairs (x_j,t_j). Together with the pair $(x_0, t_0 = \sum_i \Delta t_0^i)$, these pairs are the necessary five support points for the [2/2] rational interpolation that can be used to calculate the reciprocal differences from equations (20)-(22). Using the resulting reciprocal differences, we then have the necessary ingredients to calculate the Thiele continued-fraction interpolation using equation (23). The moveout curve obtained in this fashion, can be used either to perform a semblance analysis or to moveout correct a CMP gather.

For a single horizontal VTI layer, Douma & Calvert (2006) used 5 regularly spaced offsets to act (together with the associated traveltimes) as the support points of the [2/2] rational interpolation. For the layered case, we obtain the four* necessary p-values using a bisection approach in combination with equation (13). That is, given four offsets (or offset-to-depth ratios), we find four horizontal slownesses p_j that have offsets close to the prescribed ones (say within an accuracy of 100 m) using bisection. For a single horizontal layer this bisection approach is in principle unnecessary, since the horizontal slowness as a function of offset [derived from equation (13)] can be shown to satisfy a quartic equation that can be solved explicitly. Alternatively, we could simply use four equally spaced p_j values, with the largest p_j equal $1/\left(\max_i V_{hor}^i\right)$. This is computationally the most efficient option. We have not tested this approach, however, since we aim to stay close to the method of Douma & Calvert (2006) which obtains accurate interpolation using regularly spaced offset-to-depth ratios. Moreover, because the rational interpolation achieves high accu-

*Because the pair (x_0,t_0) simply relates to $p_0 = 0$, we need only calculate four p_j values, instead of five.

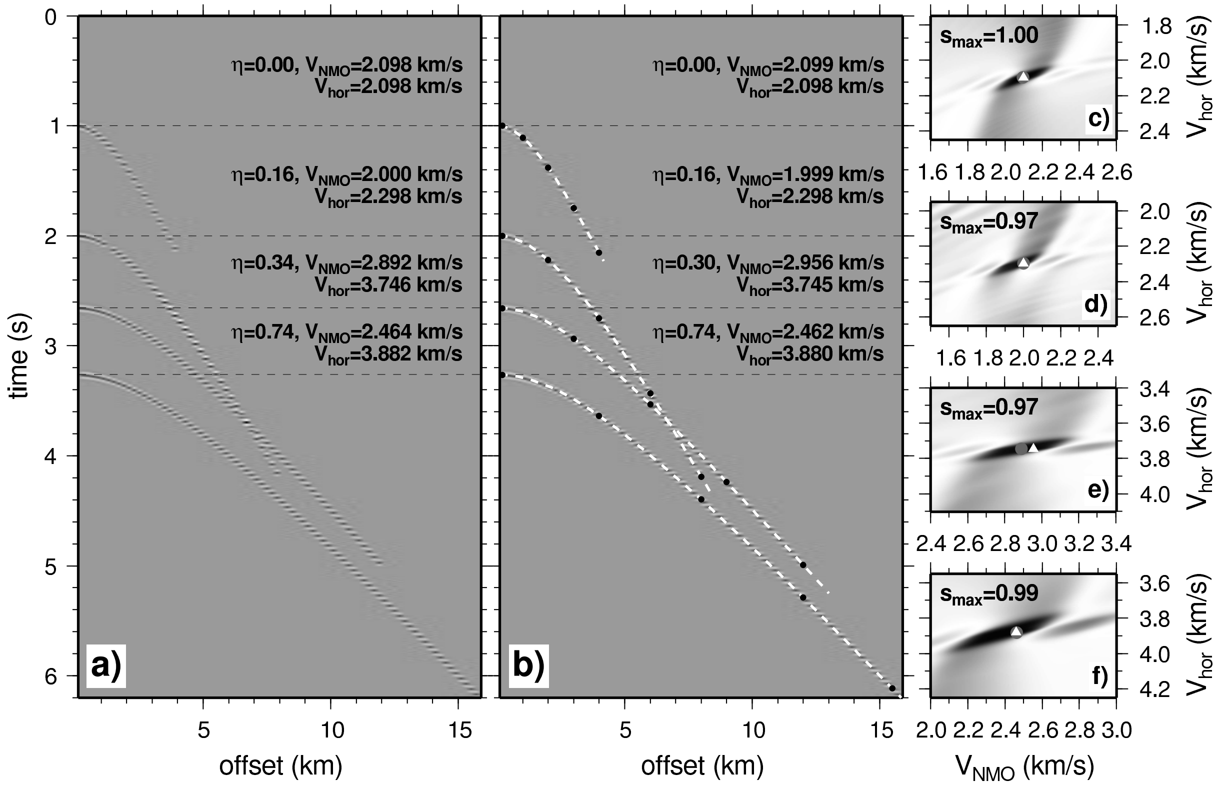

Figure 1. (a) CMP gather with qP-reflections from a 4-layer model generated using ray-tracing (see Table 1 for parameters). The layers are outlined by dashed lines, and the true values of η, V_{hor} and V_{nmo} are indicated. (b) As (a) but with estimated values of η, V_{hor} and V_{nmo} indicated together with their associated traveltimes (dashed white lines). The support points are marked by the black dots. (c-f) Semblance scans as a function of the interval values of V_{hor} and V_{nmo} for layer 1 (c) through 4 (f), respectively. The grey circles indicate the true values of associated interval values of V_{hor} and V_{nmo} while the white triangles indicate the interval values obtained from the maximum semblance ($s_{\max}$).

racy with so few support points, the computational overhead of bisection is negligible.

Since the support points are explicit in V^i_{hor}, V^i_{nmo}, and Δt^i_0, a semblance-based inversion in the x-t domain is feasible as a function of the three parameters t_0, V^i_{nmo}, and V^i_{hor}. In this way the best-fit values of V^i_{hor} and V^i_{nmo} can be determined as a function of t_0, by finding the maximum semblance combinations of V^i_{hor} and V^i_{nmo} as a function of t_0. For pure-mode qSV waves in the absence of cusps, a similar semblance analysis is feasible based on the three relevant parameters t_0, σ_i, and $V^i_{nmo,SV}$, where σ_i denotes the interval σ.

In principle, a semblance-based global inversion can be set up to determine the values of V^i_{hor} and V^i_{nmo} for all layers at the same time, or by applying the inversion in a layer-stripping fashion. In practice, however, both approaches are often not desirable, because of the trade-off between V^i_{hor} and V^i_{nmo} for limited offset acquisition geometries [e.g, (Alkhalifah, 1997; Grechka & Tsvankin, 1998)]. This tradeoff makes the inversion sensitive to errors in the observed traveltimes caused by the presence of noise or imperfect static corrections. Because this tradeoff is reduced with increasing offset-to-depth ratio (Alkhalifah, 1997), however, such procedures could be used when larger offset-to-depth ratios (approximately four or larger) are available in the data. When such data are not available and if the layer of interest is known, the overburden can be modeled as a single layer with certain effective values of V_{hor} and V_{nmo} [e.g., Tsvankin (2001, section 4.1.3)]. Once these values are established, the values of V^i_{hor} and V^i_{nmo} can be estimated by finding the maximum semblance value over a range of values of V^i_{hor} and V^i_{nmo}, while keeping the effective values of V_{hor} and V_{nmo} of the overburden fixed. This method would reduce the problem of error-propagation in a layer-stripping approach when large offset-to-depth ratios (say ≥ 3) are not available in the data.

Numerical example

Douma & Calvert (2006) applied the [2/2] rational interpolation method for a single horizontal VTI layer to a layered model to obtain effective value of η and V_{nmo}. Here, we test our method for interval parameter esti-

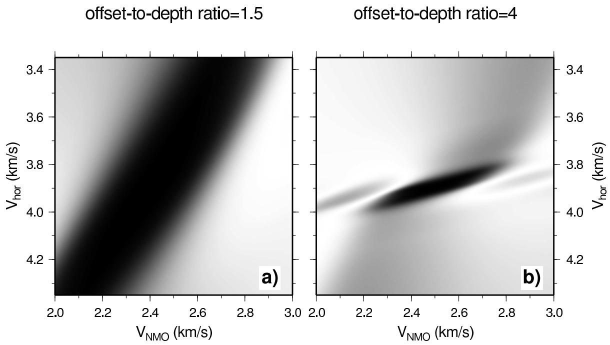

Figure 2. Semblance scans as a function of the interval values of V_{hor} and V_{nmo} for layer 4 for an offset-to-depth ratio of 1.5 (a) and 4 (b).

mation of η and V_{nmo} using the same layered model that Douma & Calvert used. The model parameters are given in Table 1. Figure 1a shows a CMP gather for this model. The top layer is elliptically anisotropic, i.e., $\eta = 0$, whereas the remaining layers have subsequently increasing values of η. The values of V_{nmo}, V_{hor}, and η for each layer are listed in Figure 1a. The level of anellipticity for the third layer (i.e., $\eta = 0.34$) can be considered high, whereas the anellipticity in the fourth layer (i.e., $\eta = 0.74$) is extreme. The values of V_{nmo}, V_{hor}, and η, for the second layer, correspond to the model parameters used in Figures 1 and 2 of Grechka & Tsvankin (1998)†. For the third and fourth layer, the model parameters correspond to a shale under zero confining pressure, and to Green River shale, respectively, [see Table 1 in Thomsen (1986) for these two cases]. Hence, even though the anellipticity in the third and fourth layer are high, they have been observed in laboratory measurements.

The CMP gather shown in Figure 1a was obtained using anisotropic ray-tracing and subsequently setting all amplitudes to 1.0. Hence, realistic amplitude and phase variations with offset are not modeled in this gather. It is known that semblance based methods can to some extent suffer from amplitude variations with offset [e.g., Sarkar *et al.* (2002)]. Here, we eliminate this complication in order to focus our attention on the ability of the proposed method to accurately determine the interval parameters of V_{nmo}, V_{hor}, and η from the traveltimes in CMP gathers.

We want to highlight that the proposed method is accurate up to large offset-to-depth ratios. Therefore, for all events in Figure 1a, the maximum offset-to-depth ratio is four. Knowing that for such large ratios the tradeoff between V_{nmo} and V_{hor} is small, we employ the proposed method in a layer-stripping setting. Figures 1c-f show the semblance scans from the

†These parameters were originally chosen because such values of η were observed on field data (Alkhalifah *et al.*, 1996).

Table 2. Effective values of V_{nmo}, V_{hor}, and η for the layered model shown in Figure 1a obtained using the Alkhalifah-Tsvankin approximation. The maximum offset-to-depth ratio used to obtain these values is 1.5.

layer	V_{nmo} (m/s)	V_{hor} (m/s)	η
1	2096	2100	0.00
2	2047	2193	0.07
3	2284	2816	0.26
4	2328	2995	0.33

first through the fourth event in Figure 1a as a function of the *interval* values V^i_{nmo} and V^i_{hor}. For each layer, the semblance scans were obtained by fixing the overburden values of V^i_{nmo} and V^i_{hor} to their estimated values. Then, by varying the interval values V^i_{nmo} and V^i_{hor} in the layer of interest and calculating the traveltime curves for each combination of V^i_{nmo} and V^i_{hor} using the rational-interpolation method given above, we determined the semblance values along these curves. The location of the maximum semblance value is indicated by the white triangle, while the location corresponding to the true model values of V^i_{nmo} and V^i_{hor} is indicated by the grey circle. Note the excellent agreement between the obtained values of V^i_{nmo} and V^i_{hor} (and thus η_i) and the true interval values of these parameters (see Figure 1b), as inferred from the close proximity of the locations of the white triangle and the grey circle. Figure 1b shows the traveltime curves (calculated using the rational-interpolation approach) associated with the obtained interval values V^i_{nmo} and V^i_{hor} (white dashed lines) superimposed on the events in the CMP gather, confirming the close match between the true traveltimes and the traveltimes from the inverted interval parameters V^i_{nmo} and V^i_{hor}. This close match is confirmed by the high maximum semblance values s_{max} (shown in Figures 1c-f), indicating the excellent agreement between the actual traveltimes and the obtained traveltimes, even for the large offset-to-depth ratio of four. The support points used for the rational interpolation are indicated by the black circles.

From the shapes of the semblance scans for all layers, it follows that V^i_{hor} is better resolved than V^i_{nmo}. This can be attributed to the relatively large value of four used for the maximum offset-to-depth ratio. Indeed, larger offsets put tighter constraints on the inversion of V_{hor} than do the smaller offsets [e.g., Alkhalifah (1997)]. Figure 2 confirms this in the context of the interval value V^i_{hor}, by showing the semblance scan for the fourth layer for a maximum offset-to-depth ratio of 1.5 (Figure 2a) and 4 (Figure 2b). Note that the larger offsets do not really add any constraints on V^i_{nmo}, since V^i_{nmo} is mainly determined by the near offsets. Therefore, the small discrepancies between the true values and obtained interval values η_i are mainly caused by small deviations of the obtained values of V_{nmo} from their true values (see Figure 1). We attribute these differences to the use of the acoustic approximation to determine the support points.

Grechka & Tsvankin (1998) introduced a method to find the interval values V_{nmo}^i and η_i from the *effective* values of V_{nmo} and V_{hor} obtained from the Tsvankin-Thomsen approximation (Tsvankin & Thomsen, 1994) [later rewritten in terms of η by Alkhalifah & Tsvankin (1995)]. This approximation describes the nonhyperbolic moveout of qP-waves in a single horizontal VTI layer. The effective values of V_{nmo} and V_{hor} are obtained by finding the best-fit values of V_{nmo} and V_{hor} using this approximation on a CMP gather containing data from a (horizontally) layered VTI medium. Because this approximation lacks accuracy at larger offset-to-depth ratios and as a result introduces a bias in the estimated values of η, we compare the proposed method to that of Grechka & Tsvankin (1998, equations (14), (16) and (17)) for a maximum offset-to-depth ratio of 1.5 only. Table 3 summarizes the results, while Table 2 shows the effective values of V_{nmo}, V_{hor} (and η) used to calculate the interval estimates shown in Table 3; the effective values were obtained through a (maximum) semblance analysis based on the Thomsen-Tsvankin approximation (Tsvankin & Thomsen, 1994) for a single horizontal VTI layer. In Table 3 the heading "GT" denotes the method by Grechka and Tsvankin, while the heading RI denotes the proposed method based on rational interpolation. The proposed method achieves higher accuracy in the interval values V_{nmo}^i, V_{hor}^i, and η^i than does the method of Grechka and Tsvankin, even for high to extreme levels of anellipticity. The small deviations of V_{hor}^i (and thus η^i), obtained with the rational-interpolation method, from their true values, are due mainly to the lack of resolution in the horizontal velocity of the data for small offset-to-depth ratios in combination with the use of the acoustic approximation in deriving equations (13) and (14).

Discussion

Rational approximations have achieved relatively accurate traveltime approximations both here and in previous studies. In light of the reported accuracy and efficiency, it therefore seems reasonable to speculate that the underlying functional dependence of the traveltime curves in layered VTI media is close to rational. This would explain the high accuracy of the proposed method with only few (here five) support points.

Rational interpolation can be accompanied by the presence of (nearby)[‡] unwanted poles on (or near) the interval of interpolation [e.g., Berrut & Mittelman (1997, p.357) or Berrut & Mittelman (2000)]. Such poles occur when the denominator becomes close to zero away from the support abscissas x_i. After the reciprocal differences in the Thiele continued fraction are calculated, the presence of such poles can easily be verified by checking for zeroes in the denominator of the corresponding [2/2] rational approximation. Also, because in the absence of nearby poles in the complex plane the derivative of the traveltime curve should always be positive in layered VTI media, the presence of such poles can be detected by checking for a change in sign of the derivative of the rational approximation $t(x)$. In case a pole is identified, the support points can be perturbed slightly using noise injection (i.e., small perturbation of the support points), to remove the pole. Alternatively, support points at different offsets (x_i) can be used. In the unlikely event that the poles are persistent under these perturbations, the rational interpolation could be replaced with a cubic spline interpolation, at the cost of the need for more support points to obtain (sub-millisecond) accuracy comparable to that of the [2/2] rational interpolation. In this work we have not observed the presence of such unwanted poles.

The presented method shows that with only few (five) support points, highly accurate traveltime curves as a function of offset can be obtained using [2/2] rational interpolation. Even though we only show its accuracy in the context of moveout analysis of qP-waves in layered VTI media, it seems worthwhile to further investigate the use of rational interpolation in more general traveltime calculations, in particular in the context of sparse storage of traveltimes. Such sparse storage is relevant in everyday seismic data processing where large traveltime tables are being used for imaging and inversion.

Conclusion

Because the horizontal slowness is preserved upon propagation through horizontally layered media, and because the traveltimes as a function of the horizontal slowness p are single-valued (i.e., no cusps), the τ-p transform is the natural domain for anisotropy parameter estimation in layered media. However, quality control of processing results and interpretation of seismic data is preferably done in the t-x domain. Based on the $\tau - p$ curve and the acoustic approximation of Alkhalifah (1998), we have presented expressions for the traveltimes and associated offsets of qP-waves in horizontally layered VTI media that are explicit in the interval values of V_{hor} and V_{nmo} and the horizontal slowness p. We have

[‡]Here, nearby is meant in the complex plane; in practice nearby would likely be defined as having a distance (in the complex plane) smaller than the smallest distance between the support abscissas x_i and x_{i+1}.

Table 3. Comparison of actual interval values of V_{nmo}, V_{hor}, and η, and the values obtained using the inversion formulas of Grechka & Tsvankin (1998) and the presented method based on rational interpolation, for a maximum offset-to-depth ratio of 1.5.

	V_{nmo} (m/s)			V_{hor} (m/s)			η		
layer	Actual	GT	RI	Actual	GT	RI	Actual	GT	RI
1	2098	2096	2098	2098	2100	2096	0.00	0.00	0.00
2	2000	1997	2003	2300	2548	2290	0.16	0.31	0.15
3	2892	2886	2918	3745	3721	3733	0.34	0.33	0.32
4	2460	2511	2490	3880	3583	3851	0.74	0.52	0.70

shown that using these expressions in combination with an $x - t$ based rational interpolation procedure, leads to highly accurate moveout curves for qP-waves in horizontally layered VTI media. These curves are in turn used to set up a three-parameter semblance analysis in the $x - t$ domain for the estimation of V_{nmo} and V_{hor} (and thus η) as a function of t_0. This method overcomes the need to process the data in the τ-p domain or to pick traveltimes in the x-t domain, as in the method of van der Baan & Kendall (2002). The presented method extends the rational interpolation based method of Douma & Calvert (2006), which is valid for a single horizontal VTI layer, to horizontally layered VTI media. Since this method naturally encompasses the single-layer case, it removes the need for the tabulated approach used by Douma & Calvert (2006). The efficiency of the method stems from the fact that only few (four) support points need to be calculated to achieve highly accurate moveout curves with rational interpolation.

ACKNOWLEDGMENTS

The anisotropic ray-tracing used to calculate the traveltimes for the events in the CMP gather of Figure 1a, was done using the ANRAY raytracing package from the Seismic Waves in Complex 3D Structures (SW3D) consortium project at Charles University in Prague (http://sw3d.mff.cuni.cz/).

REFERENCES

Alkhalifah, T. 1997. Velocity analysis using nonhyperbolic moveout in transversely isotropic media. *Geophysics*, **62**, 1839–1854.

Alkhalifah, T. 1998. Acoustic approximations for processing in transversely isotropic media. *Geophysics*, **63**, 623–631.

Alkhalifah, T., & Tsvankin, I. 1995. Velocity analysis for transversely isotropic media. *Geophysics*, **60**, 1550–1566.

Alkhalifah, T., Tsvankin, I., Larner, K., & Toldi, J. 1996. Velocity analysis and imaging in transversely isotropic media: methodology and a case study. *The Leading Edge*, **15**, 371–378.

Baker, G.A. Jr. 1975. *Essentials of Padé Approximations*. Academic Press, Inc., New York.

Bender, Carl M., & Orszag, Steven A. 1978. *Advanced Mathematical Methods for Scientists and Engineers*. New York, NY: McGraw-Hill.

Berrut, J.-P., & Mittelmann, H. 1997. Matrices for the direct determination of the barycentric weights of rational interpolation. *J. Comput. Appl. Math.*, **78**, 355–370.

Berrut, J.-P., & Mittelmann, H. 2000. Rational interpolation through the optimal attachment of poles to the interpolating polynomial. *Numer. Algorithms*, **23**, 315–328.

Chapman, C. 2004. *Fundamentals of Seismic Wave Propagation*. Cambridge University Press.

Dix, C.H. 1955. Seismic velocities from surface measurements. *Geophysics*, **20**, 68–86.

Douma, H., & Calvert, A. 2006. Nonhyperbolic moveout analysis in VTI media using rational interpolation. Accepted for publication in *Geophysics*.

Fomel, S. 2004. On anelliptic approximations for qP velocities in VTI media. *Geophysical Prospecting*, **52**, 247–259.

Grechka, V., & Tsvankin, I. 1998. Feasibility of nonhyperbolic moveout inversion in transversely isotropic media. *Geophysics*, **63**, 957–969.

Hake, H. 1986. Slant stacking and its significance for anisotropy. *Geophys. Prosp.*, **34**, 595–608.

Hake, H., Helbig, K., & Mesdag, C.S. 1984. Three-term Taylor series for t^2 - x^2 curves over layered transversely isotropic ground. *Geophys. Prosp.*, **32**, 828–850.

Helbig, K. 1994. *Foundations of Anisotropy for Exploration Seismics*. Pergamon.

Sarkar, D., Baumel, R.T., & Larner, K.L. 2002. Velocity analysis in the presence of amplitude variation. *Geophysics*, **67**(5), 1664–1672.

Stoer, J., & Bulirsch, R. 1993. *Introduction to Numerical Analysis*. 2nd edn. Springer-Verlag.

Stovas, A., & Ursin, B. 2004. New travel-time approximations for a transversely isotropic medium. *J. Geophys. Eng.*, **1**, 128–133.

Thomsen, L. 1986. Weak elastic anisotropy. *Geophysics*, **51**, 1954–1966.

Tsvankin, I. 1996. P-wave signatures and notation for transversely isotropic media: An overview. *Geophysics*, **61**, 467–483.

Tsvankin, I. 2001. *Seismic signatures and analysis of reflection data in anisotropic media*. Elsevier Science Ltd.

Tsvankin, I., & Thomsen, L. 1994. Nonhyperbolic reflection moveout in anisotropic media. *Geophysics*, **59**, 1290–1304.

Ursin, B., & Stovas, A. 2006. Traveltime approximations for a transversely isotropic medium. *accepted for publication in Geophysics*.

Van der Baan, M. 2004. Processing of anisotropic data in the $\tau - p$ domain: I-Geometric spreading and moveout corrections. *Geophysics*, **69**, 719–730.

Van der Baan, M., & Kendall, J. M. 2002. Estimating anisotropy parameters and traveltimes in the τ-p domain. *Geophysics*, **67**, 1076–1086.

Vlaar, N.J. 1968. Ray theory for an anisotropic inhomogeneous elastic medium. *Bulletin of the Seismological Society of America*, **58**, 2053–2072.

Zhang, F., & Uren, N. 2001. Approximate explicit ray velocity functions and travel times for P-waves in TI media. *Pages 106–109 of: Expanded abstracts of the 71st Ann. Internat. Mtg. Soc. of Expl. Geophys, San Antonio, Texas, USA*.

APPENDIX A: DEGENERACY OF [2/2] RATIONAL INTERPOLATION FOR HYPERBOLIC MOVEOUT WHEN INTERPOLATING SQUARED TRAVELTIME AND SQUARED OFFSET

Replacing the traveltime t and offset x in equation (16) by the squared traveltimes T and squared offsets X and adopting the normalization $N_L(0) = T(0)$ and $D_M(0) = 1.0$ after Baker (1975, pp. 5-6), the [2/2] rational interpolation is given by

$$T(X) \approx \frac{T_0 + n_1 X + n_2 X^2}{1 + d_1 X + d_2 X^2} \quad . \tag{A1}$$

Here T_0 denotes the squared zero-offset two-way traveltime. Using four support points (X_i, T_i), we arrive at a linear system of equations for the unknown interpolation coefficients n_1, n_2, d_1, d_2, i.e.,

$$A \cdot \boldsymbol{x} = \boldsymbol{d} \, . \tag{A2}$$

where

$$A \;:=\; \begin{pmatrix} -X_1 & -X_1^2 & X_1 T_1 & X_1^2 T_1 \\ -X_2 & -X_2^2 & X_2 T_2 & X_2^2 T_2 \\ -X_3 & -X_3^2 & X_3 T_3 & X_3^2 T_3 \\ -X_4 & -X_4^2 & X_4 T_4 & X_4^2 T_4 \end{pmatrix}, \tag{A3}$$

$$\boldsymbol{x} \;:=\; \begin{pmatrix} n_1 \\ n_2 \\ d_1 \\ d_2 \end{pmatrix}, \tag{A4}$$

$$\boldsymbol{d} \;:=\; \begin{pmatrix} T_0 - T_1 \\ T_0 - T_2 \\ T_0 - T_3 \\ T_0 - T_4 \end{pmatrix}, \tag{A5}$$

with T_0 the squared two-way zero-offset traveltime. Calculating $\det A$, we get

$$\begin{aligned} \det A \;=\; & X_1 X_2 X_3 X_4 \\ & [\,(T_1 T_2 + T_3 T_4)\,(X_1 - X_2)\,(X_3 - X_4) \\ & + (T_1 T_2 + T_3 T_4)\,(X_1 - X_2)\,(X_3 - X_4) \\ & - (T_1 T_2 + T_3 T_4)\,(X_1 - X_2)\,(X_3 - X_4)\,]. \end{aligned} \tag{A6}$$

When the moveout is hyperbolic, we have $T_i = T_0 + X_i/v^2$. Using this, it follows that

$$X_i - X_j = v^2\,(T_i - T_j) \ . \tag{A7}$$

Using equation (A7) in (A6), it then follows that

$$\det A = 0 \, . \tag{A8}$$

Hence, if rational interpolation is done through support points expressed as squared traveltime and squared offset, the linear system (A2) for [2/2] rational interpolation becomes degenerate in the case of hyperbolic moveout.